Structural and Functional Analysis of Violaxanthin De-Epoxidase

KUO GUO

Master Thesis:
2012-2013

Supervisor: Hans-Erik Åkerlund
Erik Hallin

Department of
Biochemistry and
Structural Biology
Lund University

Abstract

Non photochemical quenching (NPQ) is an important way for plants to protect themselves from photooxidative damage. In higher plants, the major and most rapid part of NPQ is qE, which is controlled by the Violaxanthin de-epoxidase (VDE) and zeaxanthin epoxidase (ZE). VDE converts Violaxanthin (Vx) to Antheraxanthin (Ax), and then to Zeaxanthin (Zx). Several experiments were carried through to analyze functional and structural properties of VDE. All the 13 Cysteines (Cys) in VDE were mutated to Serine (Ser) to detect the Cys that contribute to VDE activity. 12 mutations were found with decreased VDE activity. The function of the region between the N-terminal domain and the lipocalin domain was investigated by expression of the peptide before and after the linker region in different lengths combination and followed activity measurement. The results showed that the two independent domains lost majority of activity and N-terminal part of linker region was more important for activity. An experiment was set up to analyze the function of C-terminal by measuring the activity of VDE after cleaving different length of C-terminal. The result showed different degrees of activity loss that was caused by removal of different lengths of the C-terminal. A number of experiments suggests that VDE acts as a dimer that is formed at low pH. These experiments will contribute to further research of the function and structure of VDE.

Introduction

Photosynthesis is one of the most important biochemical processes in nature; the energy generated from this process has supported the majority of consumption of the living creature on this planet. The absorption of light energy by antenna pigments and the transmission of excited energy to reaction center photosystem I (PSI) and photosystem II (PSII) are the primary steps of photosynthesis. Like the raining /drought season changing in African savannah, like a several seconds shade created by a passing cloud in a sunny summer afternoon, the light quantity in natural environment never stop changing in a time scale ranges from seconds to seasons. Light is a very important environmental parameter, which to the fact that numerous of biochemical and developmental response to light have evolved in plants to help photosynthesis and growth optimization (K.K Niyogi, 2001). In their natural environment, most plants usually receive more sunlight than they actually consume for photosynthesis. Since most of plants are immobilized, it is necessary for plants to balance the absorption and utilization of light energy, and further, to minimizing the potential of photooxidative damage caused by additional absorbed light. To achieve this goal, some plants can adjust the light absorption through leaf and chloroplast movements, or even regulate the light harvesting antennae size in gene expression level (K.K Niyogi, 2001); beside such adjustment, plants also have ways to get rid of the redundant light energy which have been captured; one of those ways is so called non-photochemical quenching (NPQ) which can quench singlet-excited chlorophylls (Chl) and dissipate the excess excitation energy as heat (see Figure 1).

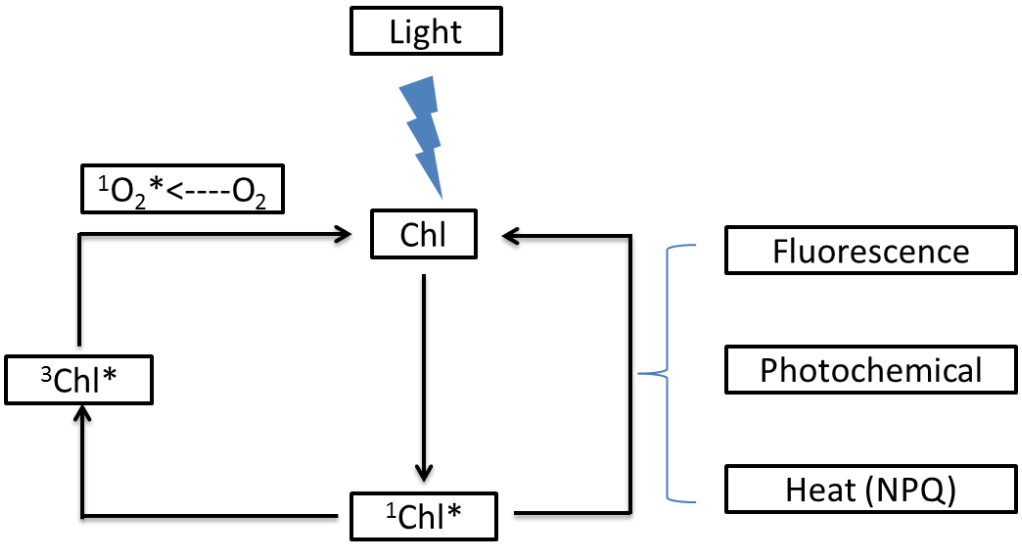

Figure 1. Various way of deexcitation of excited Chl. When ^{1}Chl is formed by Chl absorbed light, in order to go back to ground state, it can either produce ^{3}Chl* and then produce $^1O_2$*, a very reactive oxygen species; or release the energy into light (seen as fluorescence), provide energy to photosynthetic reaction, or dissipate into heat(NPQ).*

Previous research showed according to different relaxation kinetics in darkness and response to different inhibitors, NPQ can at least be divided into three parts: the major and most rapid component, qE; a second component, qT; and the third component, qI (Horton and Hague, 1988). The previous research also showed that the activation of qE requires a low lumen pH which can be generated by photosynthetic electron transport (Gilmore and Yamamoto, 1992). From previous results, a xanthophyll cycle was found in all organisms that has qE. Today, two different xanthophyll cycle has been discovered. Violaxanthin cycle exists in plants, green algae and brown algae; it is a pH dependent conversion cycle, from violaxanthin (Vx) to antheraxanthin (Ax), and then to zeaxanthin (Zx) at low pH and convert back from Zx to Vx at high pH. Diadinoxanthin cycle exists in diatoms and other eukaryotic algae; the conversion process in this cycle is between diadinoxanthin and diatoxanthin (Yamamoto et al. 1962).

The violaxanthin cycle is catalyzed by two enzyme, violaxanthin de-epoxidase (VDE) and zeaxanthin epoxidase (ZE) (see figure 2). ZE catalyze the epoxidation reaction that converts zeaxanthin to violaxanthin. VDE is a 43-kDa nucleus-encoded protein and located in lumen. It converts from violaxanthin via antheraxanthin, finally to zeaxanthin (Bugos and Yamamoto, 1996). Previous research illustrated that VDE can associate with the thylakoid membrane when lumen has been acidified (Hager and Holocher, 1994), in thylakoid membrane, VDE can interact with its substrate violaxanthin. Bratt et al (1995) also showed that VDE use ascorbic acid to reduce the epoxide group of violaxanthin.

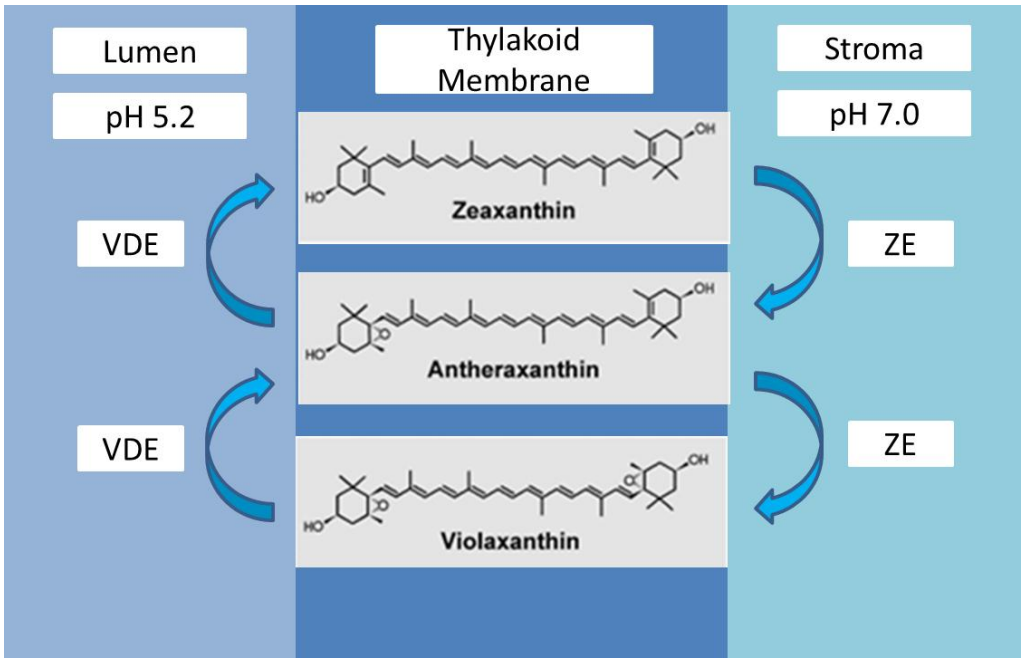

Figure 2. Overview of violaxanthin cycle. In lumen, at low pH (pH 5.2), VDE converts violaxanthin to Zeaxanthin, the reaction requires ascorbate acid as reductant; while in stroma, at pH 7.0, ZE converts zeaxanthin back to violaxanthin.

Researches of our group were mainly focused on VDE from spinach. The previous experimental work has successfully cloned spinach VDE sequence (without signal peptide) into the *Escherichia coli* (*E. coli*) Top10 strain, the expression product (VDE3) had 1 amino acid (Methionine,Met) extra in N-terminal compared to normal spinach VDE. From bioinformatics analysis result, VDE3 can be separated into three parts (Figure 3). The Cys-rich N-terminal domain which contains 11 Cysteines only exists in VDE family and has no homologous sequence in other known protein families. The previous research had illustrated that the Glu-rich C-terminal might be protonated in low pH environment and contributed to thylakoid membrane binding process (Bugos and Yamamoto, 1996). A lipocalin domain is between the previous two domains. Arnoux et al (2009) have considered such domain as a substrate binding region, their group also crystalized a non-active structure of lipocalin domain.

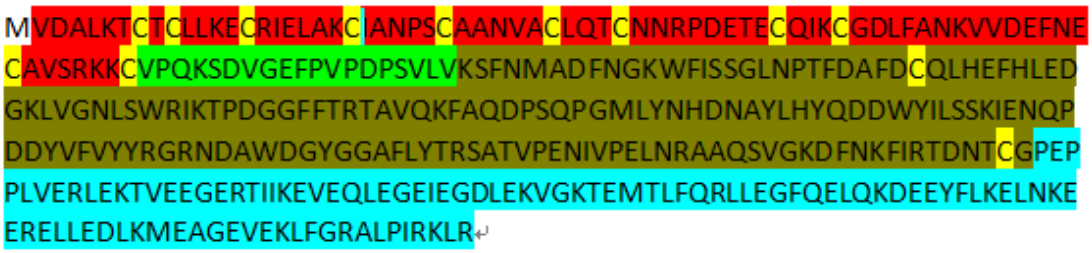

Figure 3. The VDE3 sequence. White: extra Met. Red region: N-terminal domain. Green region: suspected linker region. Dark green region: lipocalin domain. Cyan region: C-terminal domain. Amino acid marked in yellow: Cysteine.

Between N-terminal domain and lipocalin domain (Figure 3), a 19 amino acids region shows less conservation among VDE family. The bioinformatics analysis showed such region might be a random coil part and shows less conserved among VDE. The function of this peptide still remains unknown, and we suggested such peptide may work as a linker region that connects the two domains and has no contribution to VDE activity. A series of experiment had set up by our group to investigate the function of this linker region. Firstly, three points on this peptide were determined as cleavage sites; corresponding to each cleavage site, two peptides were cloned and expressed separately, and the expression products corresponding to every cleavage point were mixed together and applied to activity measurement. The result of activity assay provided evidence of ability of independent accurate refolding of the two domains beyond linker region. On the other hand, a Tobacco Etch Virus (TEV) protease cleavage site was fused to the linker region by using two-step PCR, the fusion protein was expressed and applied to activity measurement, after assured it was active, the fusion protein was cleaved into two part by using TEV Protease, the two independent active domains were acquired. The results from our experiments showed it might remain a little activity in some peptide combination, but in general, the two domains without linker part were almost impossible to form active structure independently; the low active TEV-site fusion VDE and the non-active peptide combination also showed part of the linker region was important for VDE3 activity.

In 1981, R.B. Silverman discovered that vitamin K epoxide reductase use cysteine as active site to process epoxidation activity. Previous researches have not identified the active site. There are 13 cysteines (Cys) in VDE, 11 Cys in N-terminal region and 2 in lipocalin domain; hence it is meaningful to investigate if any cysteine works as active cite which means the removal of such Cys will give absolute non-active mutant. To test the function of Cys, all Cys has been mutated to serine (Ser) one by one by our group using 2-step PCR method. By measuring the activity change of all mutants, Cys which contributes to VDE function has been determined. The activity measurement results from our experiments showed that all Cys except the first one (position Cys08) are necessary for the activity. Mutation of those 12 Cys will dramatically decrease the activity, but whether the cysteines influence the VDE activity in structural or functional way is still unknown.

According to research from H.Y. Yamamoto et al (2001), deletion of part of C-terminal of VDE will not influence activity. Three different peptide lengths have been examined by our group to find how far distance can be deleted from C-terminal end and give no influence on VDE activity. By measuring activity of the three expression products, the shortest active VDE peptide can be identified. Our experiment result showed that the removal of last 71 amino acids of VDE will keep 20% VDE3 activity, and further more cleavage decrease the activity rapidly.

The lipocalin domain structure obtained by Arnoux's group (Arnoux et al, 2009) showed at low pH, the domain exists in dimer-form, a peak shift was witnessed by us in diagram from Gel-filtration chromatography of VDE3 sample in two different buffers: Tris-HCl (pH 8.0) and citrate phosphate (pH 5.2). To investigate if the VDE worked as dimer-form, several experiments had been processed by our group. The activity of the purified Cys11 mutant, purified VDE3 and their 1:1 mixture have been measured (by using HPLC method). The result showed activity decrease to half when purified VDE3 mixed with same amount purified Cys11 mutant compare to sample only had purified VDE3 , which support that the VDE3 should work in dimer form.

Method

Construction of expression plasmids

For testing the linker region, three groups of peptides have been determined, amplified and expressed in following steps. The sequence alignment of 11 plant species showed less conserved part in linker region, three break positions have been determined based on the result (Figure 4): site QK, site FP and site PS. Corresponding to these three sites, six peptides were expressed separately (Figure 5). Peptide L1 and L2 for site QK, peptide L3 and L4 for site FP, peptide L5 and L6 for site PS.

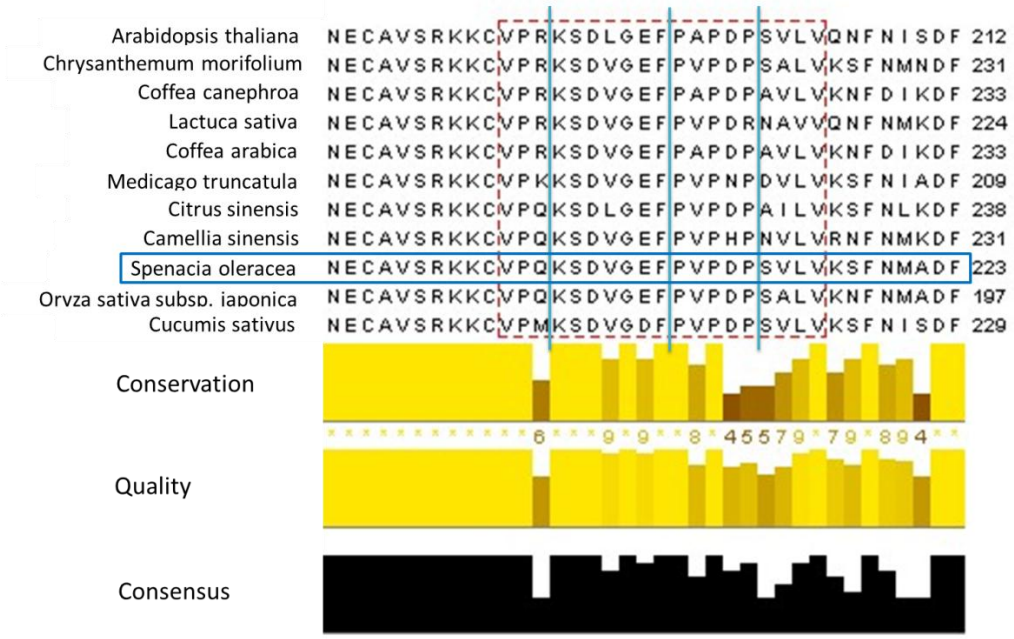

Figure 4. Sequence alignment result and cleavage sites. The linker region is marked by red square and cleavage sites (site QK, FP and PS) are marked by blue lines. On the left, the organism list of each sequence from are showed, the spinach are marked by cyan box. The conservation, quality and consensus were calculated by Jalview. Conservation: conservation of total alignment less than 25% gaps. Quality: Alignment quality based on Blosum62 scores.

The full length VDE gene (without signal peptide) has been transferred into pET22b plasmid (provided), based on the sequence, the 6 primer pairs of the sequence of 6 peptides for three break positions were designed (Table 1). The amplification and expression of target peptides were processed according to standard molecular biology methods. The recombinant plasmid were amplified in *E. coli* Top10 strain and purified, the purified plasmid was sent to eurofins mwg|operon for sequencing to assure the sequence correct. The DreamTaq DNA Polymerase, FastDigest *Nde1*, FastDigest *BamH1*, Shrimp Alkaline Phosphatase, GeneJet PCR purification Kits, GeneJet Plasmid MiniPrep Kits, GeneJet Gel Extraction Kits are all from Fermentas.

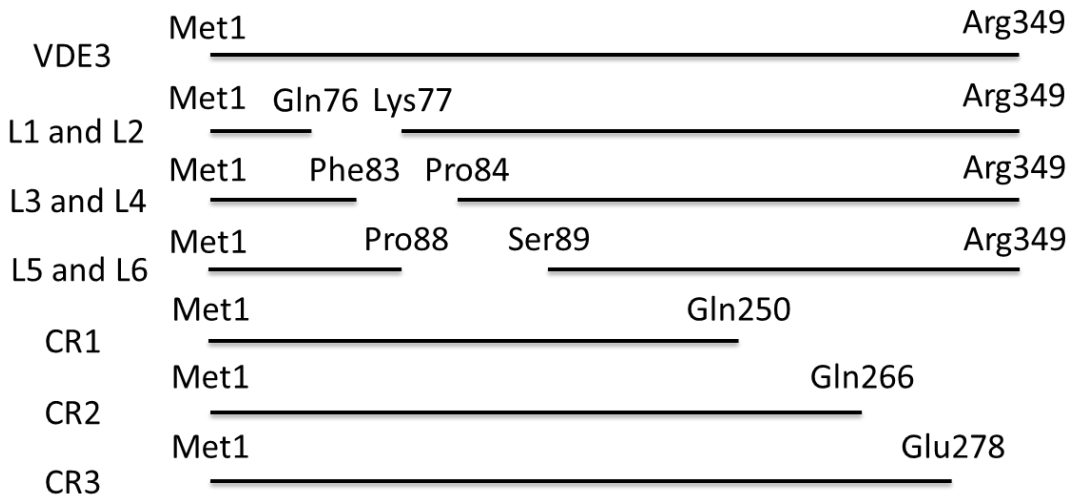

Figure 5. Sequence of constructs peptides. The figure only shows the beginning and ending amino acids with position. The expressed proteins are represented by black lines. For peptide L2, L4 and L6, the extra Met in N-terminal are not shown. The length comparison between the construct peptides and VDE3 was showed in length of the lines. The lengths of the lines are not in scale.

In order to test shortest active peptide, three different lengths of peptide were determined; these peptides were all deleted a certain length of C-terminal sequence. They were: CR1, CR2 and CR3 (Figure 5). The designed primers for these three peptides are shown in Table 1, the cloning and expression shared same method as in linker test project.

For the Cys function project and the fusion of TEV cleavage test, the mutation was processed by using two-step PCR method and Phusion Hot Start II High-Fidelity DNA Polymerase (Fermentas). The designed primer pairs for each Cys mutation (Cys1 to Cys13) and fusion TEV protease cleavage site were shown in Table 1. The cloning and expression of all the mutants shared same method as in linker test project.

TEV protease digestion design

Figure 6 shows the building of a TEV-site fusion VDE. The digestion reaction was taken place between Gln (Q) and Glu (E) and processed by using ActTEV® protease from invitrogen. Based on the protocol, a series of reaction condition test (see result part) finally determined optimal digestion condition and environment: for each 20 µg TEV-site fusion VDE, a 150 µl reaction environment within 1 µl ActTEV® protease was need; over 90% protein was digested after overnight incubation at 30^{o}C (the bands intensity was calculated by using Gel Analyzer).

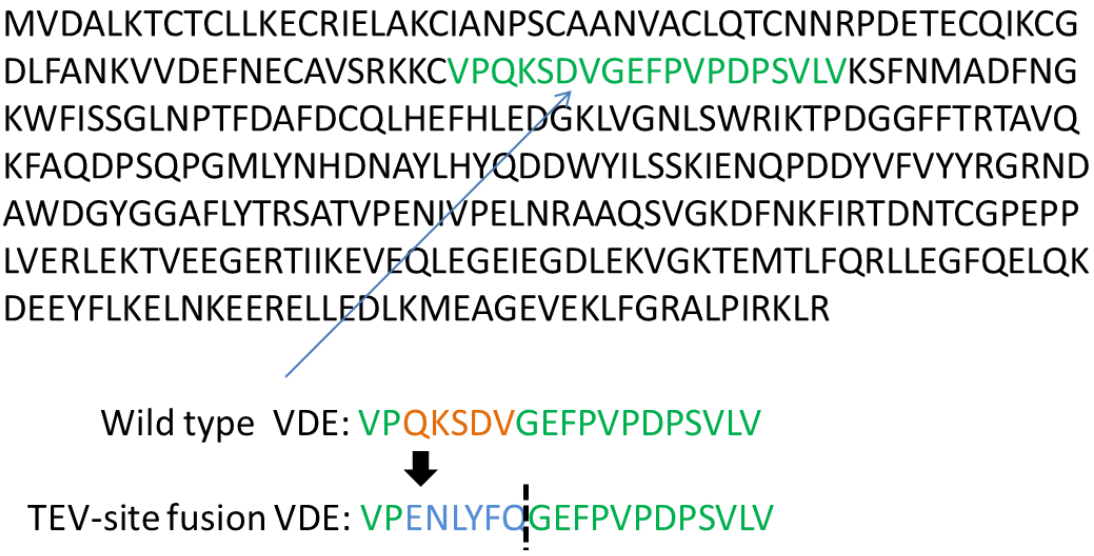

Figure 6. The fusion of TEV protease cleavage site into VDE3. The green color sequence in the black color VDE sequence is the linker part. The orange colored sequence in VDE3 will be changed into blue colored sequence to make a TEV-site fusion VDE. The cleavage site of ACTEV® protease is between Q and G (Marked in Black line).

Electrophoresis

The PCR products were identified by 1% Agarose gel electrophoresis. The DNA dye used in electrophoresis was Ethidium bromide (added into gel) or DNA-Dye NonTox provided by AppliChem (used as loading dye). The running buffer was diluted 50X TAE Electrophoresis Buffer from Fermentas. The DNA ladder was GeneRuler™ 1kb Plus DNA Ladder from Fermentas.

The protein samples were identified by using sodium dodecyl sulfate polyacrylamide gel electrophoresis (SDS-PAGE). The running buffer was diluted Mops SDS Running Buffer (20X) from invitrogen. The precast gel was NuPAGE® Novex® 4-12% Bis-Tris Midi Gel from invitrogen. The protein ladder was PageRuler™ Plus Prestained Protein Ladder from Fermentas.

Expression of target protein

The correct plasmids were amplified in *E.coli* Top10 strain, then purified and transferred to *E.coli* BL21 strain for expression. The culture condition of BL21 cells was 37°C, 200 rpm. The expression of target protein was induced by 1 mM Isopropyl β-D-1-Thiogalactopyranoside (IPTG) when OD_{600} of cell culture reach 0.6. The expression took 2 hours at 37°C and the cells collected by using centrifugation (6000 RCF, 10 min). The pellet cell was washed (100 mM Tris-HCl, 170 mM NaCl) twice.

Cell disruption and purification of expression products

The cell disruption was done by using Lysozyme combined with 0.1 mm cell disruption glass beads. The washed cell pellet were resuspended in Lysis buffer (50 mM Tris-HCl, 10mM Ethylene Diamine Tetraacetic Acid (EDTA), 1% Triton X-100, 500 mM NaCl, 5mM DL-Dithiothreitol (DTT), pH0.6), the lysozyme amount changes according to cell amount (4 mg lysozyme per 1 g cell); after 15 min incubation, same volume of glass beads as cell pallet volume were added into the mixture, the disruption cycle was: 30 sec vortex and 30 sec on-ice incubation, repeat 15 times.

The homogenates were applied to centrifugation (15 000 RCF, 15 min, 4^{o}C) and followed by 5 washing steps to purify the inclusion body, the step1-3 followed same cycle: resuspend cell pellet in buffer1 (20 mM Tris-HCl, 10 mM EDTA, 5 mM DTT, 1% Triton X-100, pH 8.0), and apply to centrifugation (15 000 RCF, 15 min, 4^{o}C); for step 4, cell pellet was resuspended in buffer2 (20 mM Tris-HCl, 10 mM EDTA, 5 mM DTT, pH 8.0), and applied to centrifugation (15 000 RCF, 15 min, 4^{o}C); for step 5, cell pellet was resuspended in buffer3 (20 mM Tris-HCl, 10 mM EDTA, 5 mM DTT, 8 M urea, pH 8.0), and incubated for 1 hour with magnetic stirrer, then applied to centrifugation (15 000 RCF, 30 min, 25^{o}C), the supernatant of step5 was purified solubilized inclusion body.

A refolding processed followed the washing steps to reactivate unfolded protein. The refolding process was done by using PD-10 Desalting column from GE healthcare, the desalting steps followed the protocol of PD-10 column in total 2 cycles, urea and DTT was removed one by one in those continues cycles, the component of washing buffer in cycle1 was 20 mM Tris-HCl pH8.0, 10 mM EDTA, 5 mM DTT; in cycle2, the buffer component was 20 mM Tris-HCl pH8.0, 10 mM EDTA. While desalted protein sample eluted from column in the last cycle, the protein sample was mixed with 2 mM oxidized Glutatione (GSSG) and 0.3 mM reduced Glutatione (GSH) and incubated overnight to allow protein oxidation in redox buffer. The refolded protein was applied to gel-filtration chromatography to isolate the active component from missfolded and aggregates. The collection from gel-filtration chromatography was applied to concentrating steps (by using Vivaspin 15R tubes from Sartorius stedim biotech) to get a high concentration protein sample.

Activity assay

Activity measurements were based on dual-wavelength measurements (A_{502}-A_{540}) according to Yamamoto and Higashi (1978). The measurements were processed on UV-3000 spectrophotometer. The measurement condition was citrate buffer (50 mM citric acid, 110 mM Na_2HPO_4, pH 5.2), the substrate was 0.33 µM Violaxanthin and 9

µM Monogalactosyldiacylglycerol (MGDG), 30 mM Ascorbate was added after VDE incubated with substrate in buffer for 3 min to start the reaction.

Activity measurement by using HPLC

For some low activity protein sample, the dual-wavelength method could not detect its activity; a new method was applied to detect how much violaxanthin can be converted to zexanthin by certain protein sample. The conversion was measured by using High Performance Liquid Chromatography (HPLC) with C_{18} HPLC column from Agilent Technologies. The preparation of loading sample was as follows: a 200 µl reaction system was set up, with 20 µl Violaxanthin and MGDG mixture (66 µM Violaxanthin and 1.8 µM MGDG), 20 µl protein sample, 6 µl 1 mM Ascobate and 154 µl H_2O; after 1 hour incubation, the reaction was stopped by using 3.5 µl NaOH, 800 µl Acetone was added to the reaction solution to extract pigments and centrifuge at 13 200 RCF for 10 min to pellet down insoluble component; in order to make sure no insoluble particle will load into column, a repeat centrifugation will applied to the previous supernatant. To increase to polarity, 150 µl H_2O was added into Acetone solution before loading. For linker sample (L1 to L6), due to their low activity, the measurement was done by use non-diluted sample; as for measurement of VDE and Cys11 mixture (for dimerization research), the VDE was diluted 12 000 times to lower the reaction speed into an 1 hour time scale, the Cys11 sample was diluted to the same concentration as VDE.

Gel-filtration chromatogram

The analytical and purification-purpose gel-filtration chromatography column were packed with Sephacryl S-200 material (from GE healthcare). The packing steps of analytical column were followed protocol provided by GE healthcare. For larger scale purification of expression products, a HPLC system was connected with a prepacked Sephacryl S-200 column (from GE healthcare).

Table 1. Sequence of primer pairs for peptides constructs.

Linker test project		Primer pair 1 (5'---->3')	Primer pair 2 (5'---->3')
	Cleavage site QK	Sense primer: TTAAGAAGGAGATATACATATGG Anti-sense primer: GCCGGATCCTTACTGAGGCACGCATTTC	Sense primer: CGTCATATGAAGTCTGATGTTGGAGAATTTC Anti-sense primer: TTCGGATCCTTACCGAAG
	Cleavage site FP	Sense primer: TTAAGAAGGAGATATACATATGG Anti-sense primer: GCCGGATCCTTAAAATTCTCCAACATCAGAC	Sense primer: CGTCATATGCCTGTTCCCGATCCTAGTG Anti-sense primer: TTCGGATCCTTACCGAAG
	Cleavage site PS	Sense primer: TTAAGAAGGAGATATACATATGG Anti-sense primer:GCCGGATCCTTAAGGATCGGGAACAGGA	Sense primer: CGTCATATGAGTGTGCTCGTTAAGAGTTTC Anti-sense primer: TTCGGATCCTTACCGAAG
C-terminal deletion test		Primer pair (5'---->3')	
	Peptide M1 to G250	Sense primer: TTAAGAAGGAGATATACATATGG Anti-sense primer: GTCGGATCCTTACCCACAGGTATTGTCCG	
	Peptide M1 to G266	Sense primer: TTAAGAAGGAGATATACATATGG Anti-sense primer: GTCGGATCCTTATCCTTCCTCCACCGTC	
	Peptide M1 to E278	Sense primer: TTAAGAAGGAGATATACATATGG Anti-sense primer: GTCGGATCCTTATTCTAATTGTTCTACTTCCTTAA	
Cys mutation test		1st step PCR primer pair (5'---->3')	2nd step PCR primer pair (5'---->3')
	Cys08Ser (Cys1)	Sense primer1: GATGCTCTTAAAACTTCTACCTGTTTGCTGAAGG Anti-sense primer1: TTCGGATCCTTACCGAAG Sense primer2: TTAAGAAGGAGATATACATATGG Anti-sense primer2: CCTTCAGCAAACAGGTAGAAGTTTTAAGAGCATC	Sense primer: TTAAGAAGGAGATATACATATGG Anti-sense primer: TTCGGATCCTTACCGAAG
	Cys10Ser (Cys2)	Sense primer1: CTCTTAAAACTTGTACCTCTTTGCTGAAGGAATGC Anti-sense primer1: TTCGGATCCTTACCGAAG Sense primer2: TTAAGAAGGAGATATACATATGG Anti-sense primer2: GCATTCCTTCAGCAAAGAGGTACAAGTTTTAAGAG	
	Cys15Ser (Cys3)	Sense primer1: GTTTGCTGAAGGAATCCAGAATTGAACTCGC Anti-sense primer1: TTCGGATCCTTACCGAAG Sense primer2: TTAAGAAGGAGATATACATATGG Anti-sense primer2: GCGAGTTCAATTCTGGATTCCTTCAGCAAAC	
	Cys22Ser (Cys4)	Sense primer1: GAACTCGCCAAGTCCATCGCAAATCC Anti-sense primer1: TTCGGATCCTTACCGAAG Sense primer2: TTAAGAAGGAGATATACATATGG Anti-sense primer2: GGATTTGCGATGGACTTGGCGAGTTC	
	Cys28Ser (Cys5)	Sense primer1: TCGCAAATCCATCTTCTGCAGCCAATGTTG Anti-sense primer1: TTCGGATCCTTACCGAAG Sense primer2: TTAAGAAGGAGATATACATATGG Anti-sense primer2: CAACATTGGCTGCAGAAGATGGATTTGCGA	
	Cys34Ser (Cys6)	Sense primer1: GCCAATGTTGCTTCCCTGCAGACCTGC Anti-sense primer1: TTCGGATCCTTACCGAAG Sense primer2: TTAAGAAGGAGATATACATATGG Anti-sense primer2: GCAGGTCTGCAGGGAAGCAACATTGGC	
	Cys38Ser (Cys7)	Sense primer1: CTTGCCTGCAGACCTCCAATAATAGACCTG Anti-sense primer1: TTCGGATCCTTACCGAAG Sense primer2: TTAAGAAGGAGATATACATATGG Anti-sense primer2: CAGGTCTATTATTGGAGGTCTGCAGGCAAG	
	Cys47Ser (Cys8)	Sense primer1: CTGATGAAACCGAATCCCAAATCAAATGTG Anti-sense primer1: TTCGGATCCTTACCGAAG Sense primer2: TTAAGAAGGAGATATACATATGG Anti-sense primer2: CACATTTGATTTGGGATTCGGTTTCATCAG	
	Cys51Ser (Cys9)	Sense primer1: GAATGCCAAATCAAATCTGGGGACTTGTTC Anti-sense primer1: TTCGGATCCTTACCGAAG Sense primer2: TTAAGAAGGAGATATACATATGG Anti-sense primer2: GAACAAGTCCCCAGATTTGATTTGGCATTC	
	Cys66Ser (Cys10)	Sense primer1: GACGAGTTCAACGAGTCTGCAGTCTCTCG Anti-sense primer1: TTCGGATCCTTACCGAAG Sense primer2: TTAAGAAGGAGATATACATATGG Anti-sense primer2: CGAGAGACTGCAGACTCGTTGAACTCGTC	
	Cys73Ser (Cys11)	Sense primer1: CTCGAAAGAAATCCGTGCCTCAGAAGTCTG Anti-sense primer1: TTCGGATCCTTACCGAAG Sense primer2: TTAAGAAGGAGATATACATATGG Anti-sense primer2: CAGACTTCTGAGGCACGGATTTCTTTCGAG	
	Cys119Ser (Cys12)	Sense primer1: GACGCTTTTGATTCCCAGTTACATGAGTTCC Anti-sense primer1: TTCGGATCCTTACCGAAG Sense primer2: TTAAGAAGGAGATATACATATGG Anti-sense primer2: GGAACTCATGTAACTGGGAATCAAAAGCGTC	
	Cys249Ser (Cys13)	Sense primer1: CGAACGGACAATACCTCTGGGCCCGAG Anti-sense primer1: TTCGGATCCTTACCGAAG Sense primer2: TTAAGAAGGAGATATACATATGG Anti-sense primer2: CTCGGGCCCAGAGGTATTGTCCGTTCG	
		1st step PCR primer pair (5'---->3')	2nd step PCR primer pair (5'---->3')
Fusion of TEV protease cleavage site		Sense primer1: CTGGAAGTACAGGTTCTCAGGCACGCATTTCTTTC Anti-sense primer1: TTCGGATCCTTACCGAAG Sense primer2: TTAAGAAGGAGATATACATATGG Anti-sense primer2: GAGAACCTGTACTTCCAGGGAGAATTTCCTGTTCCC	Sense primer: TTAAGAAGGAGATATACATATGG Anti-sense primer: TTCGGATCCTTACCGAAG

Result

Cysteine contributes to VDE activity to different extent

The sequencing results showed the DNA sequence in reconstructed plasmid matches to the designed sequence. After purification of protein samples, all samples (including mutant from 1st Cys to 13th Cys (sample number Cys1 to Cys13) and VDE3 (F1, F2 and F3)) were applied to SDS-PAGE and checked for the product size, the SDS-PAGE result are shown in Figure 7. The size of mutants and VDE3 are same, at around 40 kDa, and the bands position on the gel matched to the molecular weight.

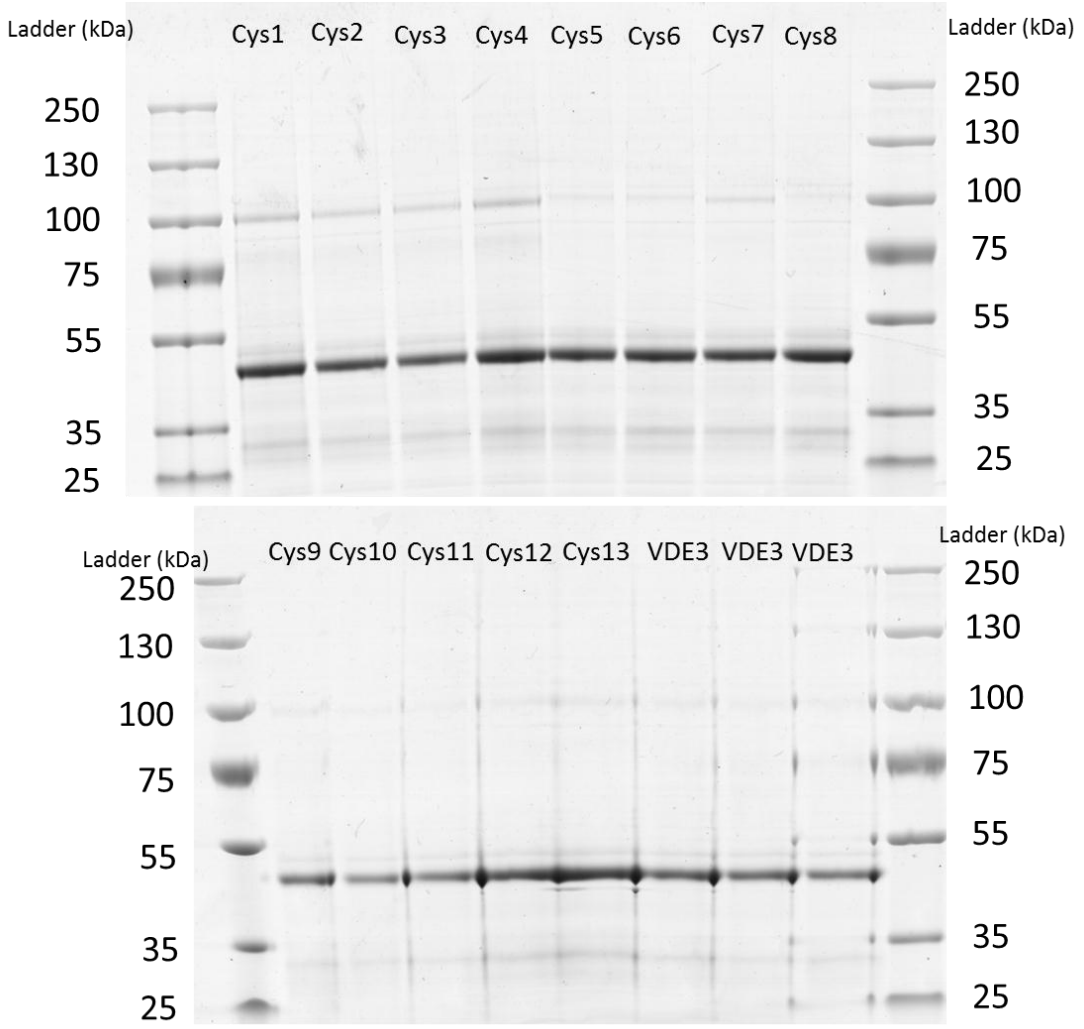

Figure 7. SDS-PAGE result of Cysteine mutant products. The size of ladders is shown in both sides. The sample name is marked in each lane, from left to right, top to bottom, were 13 mutants (sample number Cys1 to Cys13) and 3 VDE3 samples (from different batch), from sequence data, all mutants and VDE3 share same molecular mass at around 40 kDa. The shallow band at around 100kDa in each line is suspected VDE dimer bands.

The activity measurement results from dual-wavelength method are given below (Figure 8). Based on activity and protein concentration, specific activity of each mutants and VDE3 were calculated and listed in one figure. The result of activity measurements was calculated from average of three parallel measurements. The average specific activity of 3 VDE3 was set as standard (100% activity), based on standard activity, the percentage number of each mutant were calculated. The results showed except the mutant which the 1st Cys mutate to Ser (Cys1), all other mutants gave very low activity compare to VDE3. Cys1 showed much higher activity than wild type (1.5 times), for other mutants, their activity were deeply affected by Cys mutation to Ser, the most active mutant Cys8 only showed 3.5% of the wild type activity, and some mutants even showed less than 0.001% of wild type activity.

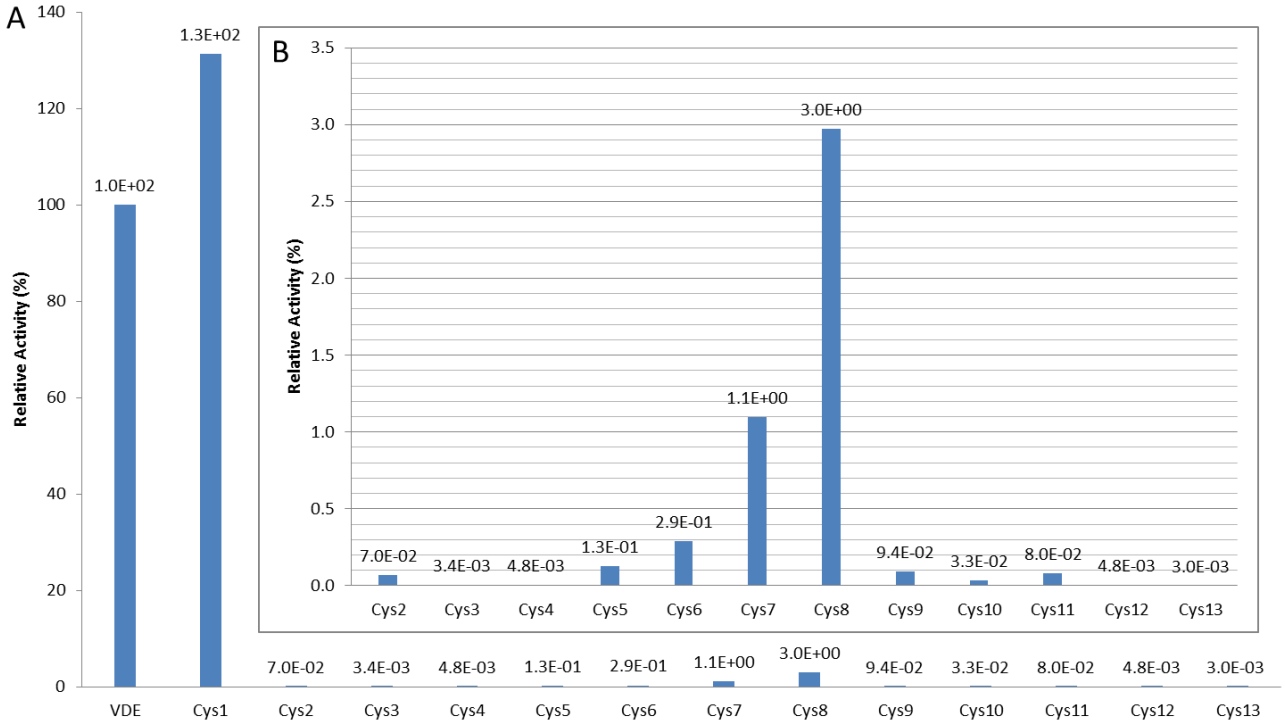

Figure 8. Relative activities of Cysteine mutants. The activity of each mutants was compared with VDE3 (F) and presented in a percentage number (relative activity) A. the overview of all mutants (Cys1 to Cys13) and average of VDE3. B. the relative activity of 12 low-active mutants.

Linker region contributes to VDE activity

In order to identify how the 6 peptide of linker project expressed in *E. coli* cell, the supernatant and pellet of the 1st centrifugation after cell disruption of each sample were applied to SDS-PAGE. The result (Figure 9) showed 3 larger size peptides (L2, L4 and L6) formed inclusion body during expression and showed three clear bands in those pellet lanes. As for the three small size peptide, they showed different expression condition, L1 was found in inclusion bodies, L3 was found in both soluble protein and inclusion bodies, while the L5 was only found in the soluble protein

fraction. Since the mass of each small peptide is less than 10 kDa, their bands position were not match to ladder, while their relative movement position in gel were still according to their mass difference, and could be visualized in the gel (marked by black arrow).

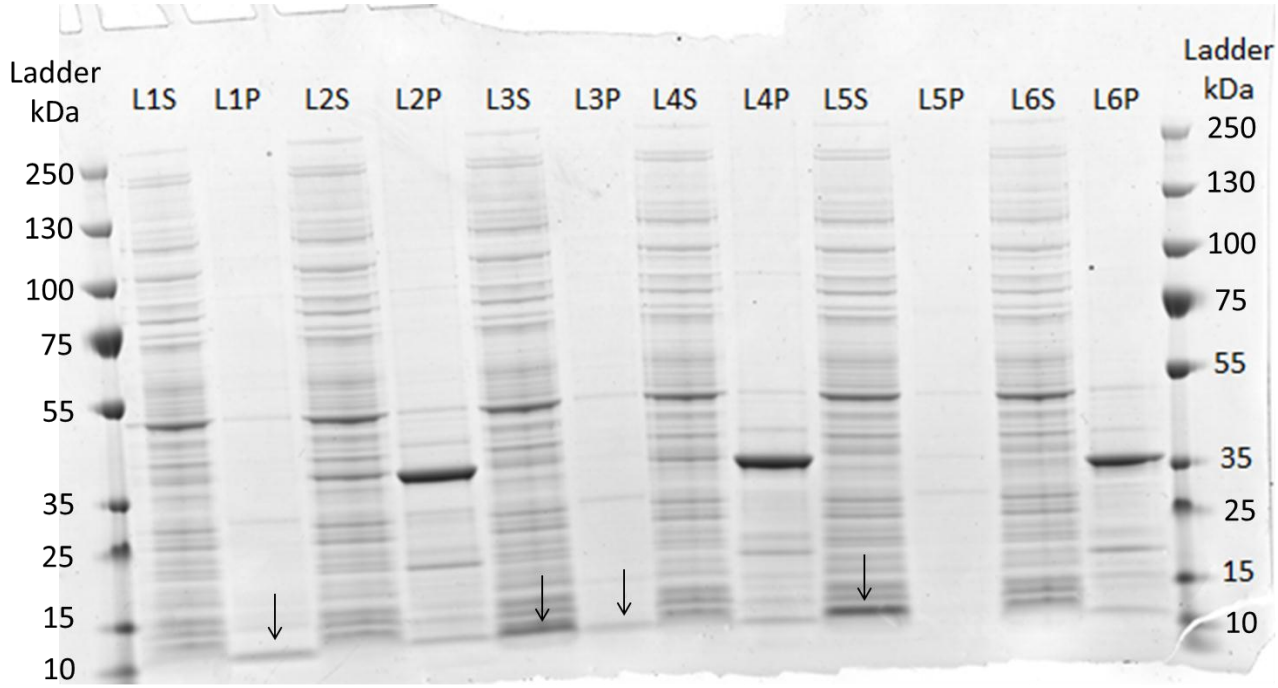

Figure 9. SDS-PAGE result of identification of arrangement of six peptide expression in E.coli. Six samples were loaded in order by number and supernatant (S) before pellet (P). The size of each sample: L1, 8.2 kDa; L2, 31.4 kDa; L3, 8.9 kDa; L4, 30.7 kDa; L5, 9.5 kDa; L6, 30.2 kDa.

The activity measurement result by using dual-wavelength method of the six peptide combination showed no activity. Another measurement by using HPLC detecting pigments conversion was applied to three combinations: L1+L2, L3+L4, L5+L6. The result was shown in Table 2. It can be seen that after 1 hour incubation, combination L1+L2 gave no conversion from Vx to Ax or Zx; combination L3+L4 converted less that 1% Vx into Ax but no conversion to Zx; and the combination L5+L6 converted more than 7% of Vx to Ax and 1.31% Vx finally converted to Zx. The background test of 6 independent peptides showed no conversion detected.

Table 2. Result of HPLC detecting different pigment amount in different sample combination. The area is calculated by the integration of peaks from the HPLC chromatogram.

	Relative Amount (%)		
Combination	Vx	Ax	Zx
L1 and L2	100.00	0.00	0.00
L3 and L4	99.63	0.37	0.00
L5 and L6	92.73	5.96	1.31

TEV site fusion VDE shows low activity

Figure 10A shows the result of digestion condition test. The calculation result from Gel Analyzer showed in lane 30°C, over 90% of VDE was digested into two peptides after overnight incubation at 30°C. The activity measurement result showed expressed TEV-site fusion VDE has very low activity (1/1000 of VDE3), and no activity was found for the digestion products. Due to the fact that 30 µM DTT in ACTEV protease restoration buffer which was enough to inhibit 130 µg/ml VDE3, 100 µM GSSG was mixed with ACTEV protease before cleavage reaction to create an oxidative state and remove the influence of DTT. While the digestion result in Figure 10B, showed overnight incubation at 30°C still gave almost no digestion products, the ACTEV protease was highly inhibited.

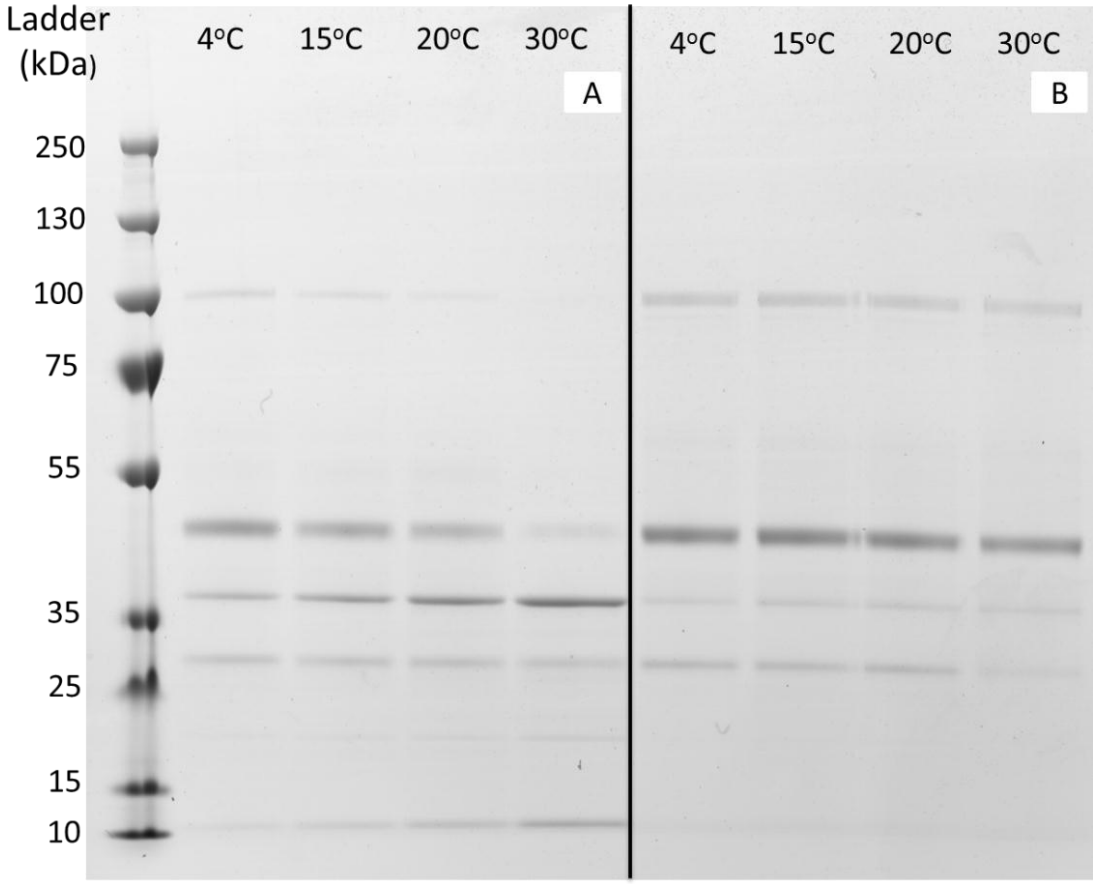

Figure 10. SDS-PAGE result of ACTEV protease digestion condition test. A. Digestion test of different incubation temperature. B. Digestion test in oxidative state. The size of different peptides in reaction solution: TEV-site fusion VDE, 40 kDa; ACTEV protease, 27 kDA; large size digestion product, 31 kDa; small size digestion product, 8.8 kDa. The band at 100 kDa position in each line is suspected dimer of fusion VDE. The band between 35 kDa and 25 kDa is ACTEV protease.

C-terminal length influences VDE activity

Figure 11 showed the SDS-PAGE of purified soluble inclusion body of expression product in C-terminal function project. By comparing with protein ladder, the bands position of 3 products matched to their expected molecular size.

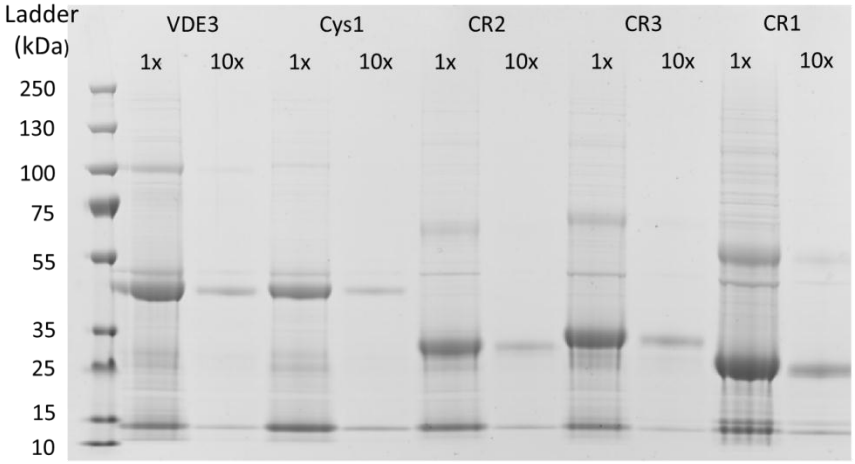

Figure 11. SDS-PAGE gel of CR1, CR2, CR3 and VDE3. For each sample, 2 different concentrations were loaded: origin dialysis products (1X) and 10 times dilution (10X). The mass of each sample: VDE3, 40 kDa; CR1, 28 kDa; CR2, 30 kDa; CR3, 31 kDa. The dimer bands can also be seen in lanes 1X of each protein sample.

The activity measurement result was shown in Figure 12. The result showed CR3 remained 20% of VDE3 activity, while the activity of CR2 and CR1 were considerably lower (2.1% and 0.19% of full activity remained).

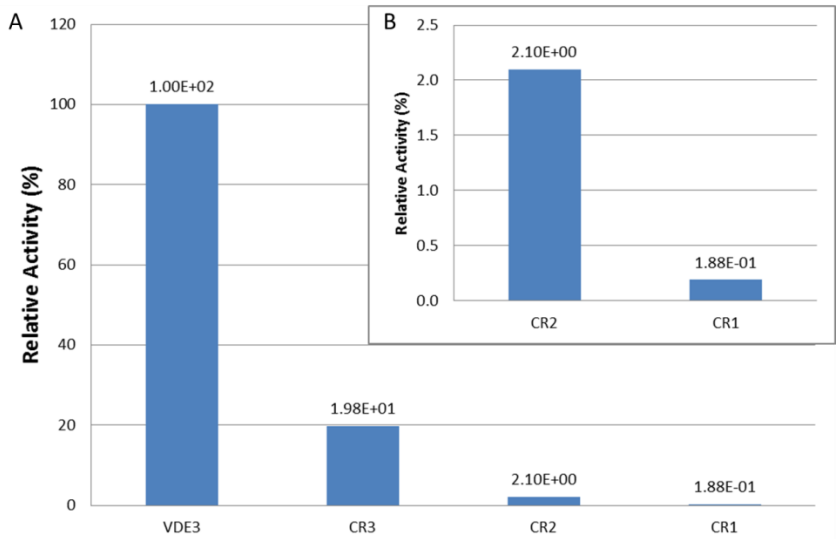

Figure 12. Relative activity of 3 different-length-C-terminal-removed peptides (CR1, CR2 and CR3) compared to VDE3 (F). A. Overview of relative activity from all samples. B. Relative activity of CR2 and CR1.

Dimerization of VDE3

Figure 13 shows the comparison of two different chromatograms in the same analytical Sephacryl S-200 column. The blue chromatogram was from 260 µg VDE loaded in pH 8.0 Tris-HCl environment; the red chromatogram was from same amount VDE3 loaded into pH 5.2 citrate phosphate buffer after incubated 30 min in the same buffer. It can be seen that a 2 ml peak shift appeared, which means the size of VDE in low pH buffer were different from in high pH buffer; which can be explained by a dimerization of VDE3 in acidic condition.

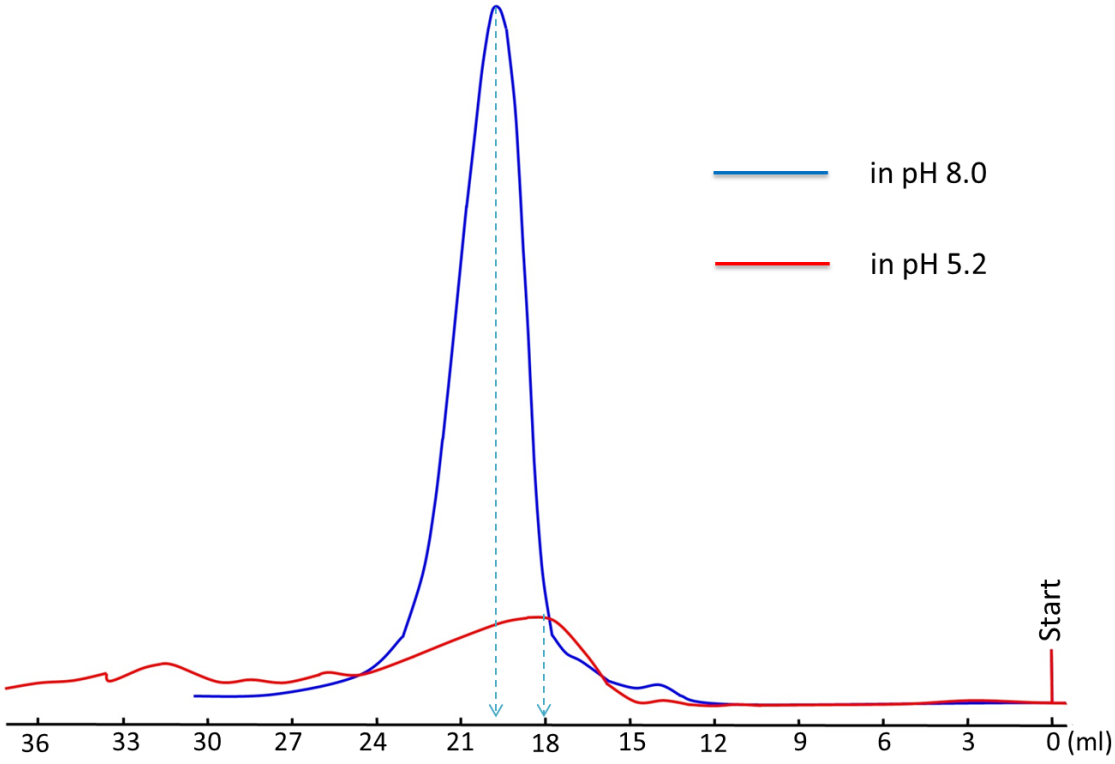

Figure 13. Chromatogram of VDE in low pH (pH 5.2) and high pH (pH 8.0). The flow speed was 0.3 ml/min. The Elution volumes of two peaks were: 18 ml (VDE in pH 5.2) and 20ml (VDE in pH 8.0)

Figure 14 A B C shows the activity measurement result of VDE3, Cys11 and their mixture by using HPLC method. The result was given by the trend of three components changed in certain time scale (1 hour). The result showed in both VDE3 sample and VDE3+Cys11 mixture, the amount of Vx decreased and Zx increased following time changing. The Cys11 sample had no component changing and no Ax or Zx was converted. The Figure 14D was the merger of two diagrams: VDE diagram and VDE+Cys11 mixture diagram, for convenient to see component changes in Vx

and Zx, curve of Ax were not shown. It can be seen in Figure 14D that the slope of curves in VDE diagram are higher than that in VDE+Cys11 mixture diagram.

Figure 14E is the merger of two diagram: VDE3 diagram was in 1 hour time scale; as for the diagram of mixture, the speed of reaction was artificially doubled by compressing the 4 measurements (7th min, 15th min, 30th min and 60th min) from 1 hour time scale into 30 minutes time scale but with same number of measurements (3.5th min, 7.5th min, 15th min and 30th min). The new made diagram of VDE3+Cys11 mixture showed almost same trend as the VDE diagram.

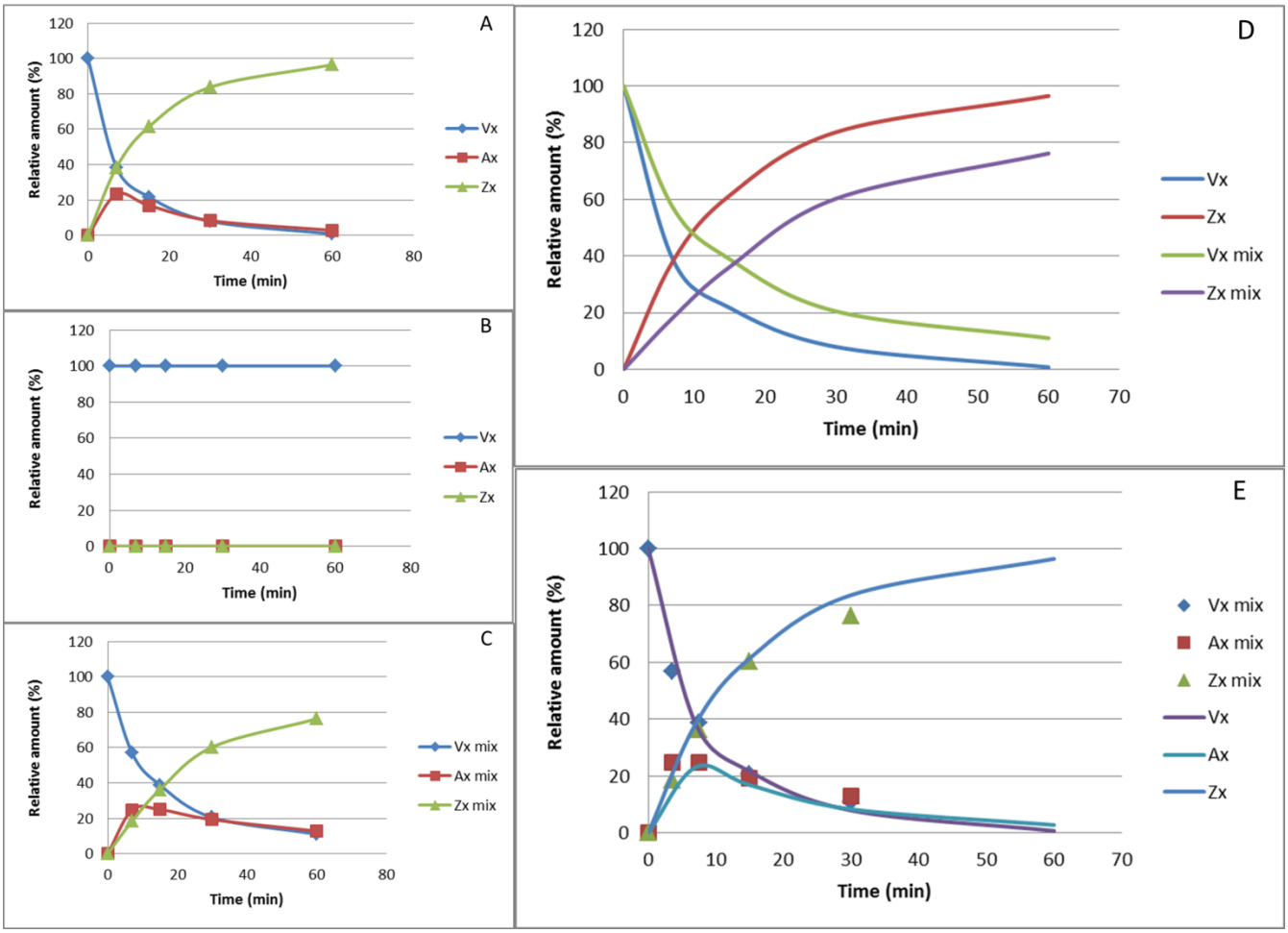

Figure 14. The diagram of activity measurement of VDE, Cys11, and their mixture by using HPLC method. All components (Vx, Ax and Zx) are shown in percentage of total amount (total integration value of peak area). Figure A, B and C are correlated to sample VDE, Cys11 and their mixture separately. Figure D is the merger of A and C without Ax curves. Figure E is merger of A and artificially modified C.

Figure 15 showed the comparison of two different chromatograms in the same purification Sephacryl S-200 column at pH 8.0 Tris-HCl buffer. The blue diagram was from refolded VDE3 inclusion body; the red diagram was from refolded C-terminal-cleaved VDE (sample CR1) inclusion body. In each chromatogram, three

main peaks can be seen. They were, in size order, aggregation peak, dimer peak and monomer peak. The activity of each peak showed only the monomer peak in VDE sample and dimer peak in CR1 sample were active.

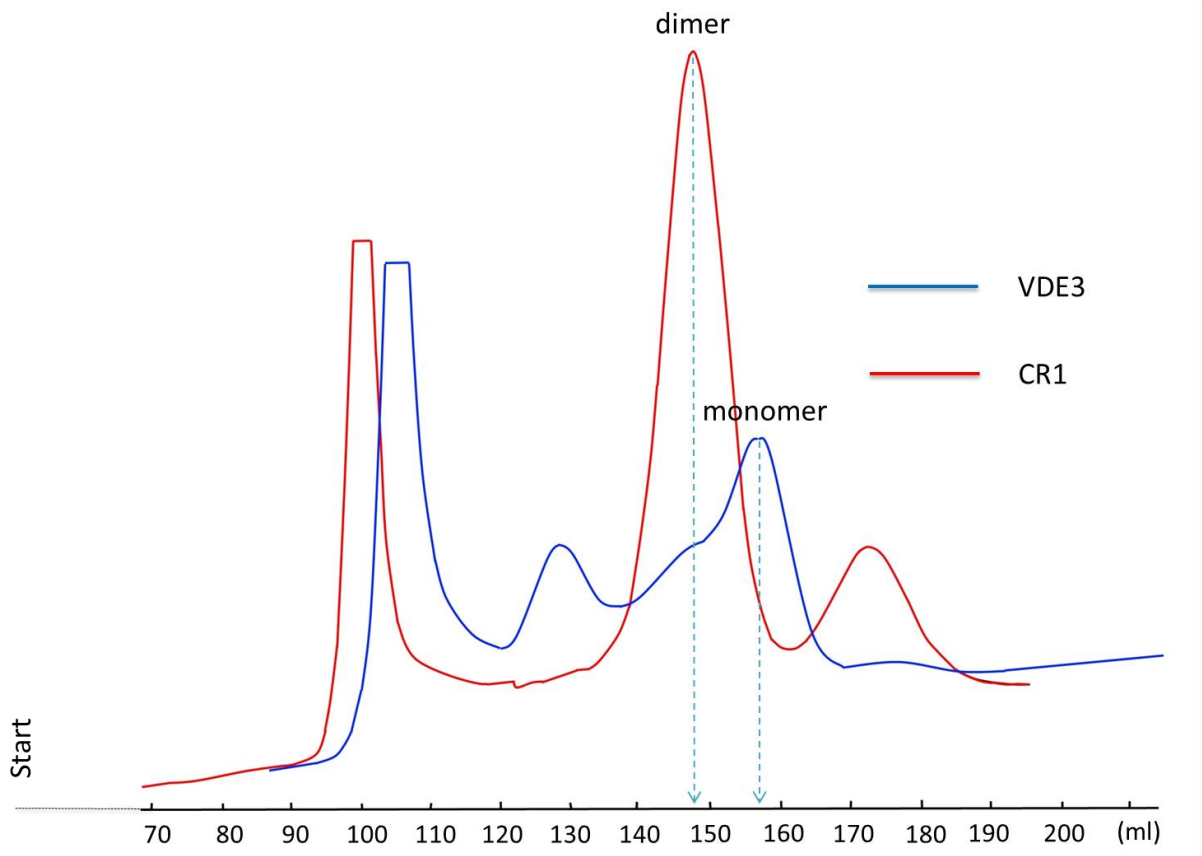

Figure 15. The chromatogram of refolded CR1 and VDE inclusion body in pH 8.0 buffer. The elution volume of CR1 dimer and VDE monomer were 148 ml and 156 ml. The size of CR1 and VDE monomer were 28 kDa and 40 kDa. The diagram before 70 ml was not shown. The starting point was used to mark diagram direction. The flow speed was 1ml/min

Discussion

The activity measurement result of different Cys mutants showed that all Cys except the first Cys were important for VDE activity. For those mutants that showed low activity, the data was from dual-wave length method, and the reading from UV-3000 spectrophotometer was close to the detection limit; thus we cannot assure if the low activity read mutants truly active.

Cys1 is the only mutant that shows higher activity than VDE3. Sequence alignment showed that Cys1 was less conserved in VDE than other Cys, e.g., Cys1 was not present in some algae species. This suggests that the Cys1 is a free Cys and has less contribution to VDE activity and structure. Another possible suggestion of Cys1 function is that it might form a disulfide bond with the Cys in signal peptide during expression. But the reason of mutant Cys1 highly increased activity still needs further research.

The two least active Cys mutants, Cys12 and Cys13 are located in lipocalin domain. From the structure of lipocalin domain obtained by Arnoux's group (Arnoux et al, 2009), the two Cys are close in spatial position, illustrated that they might form a disulfide bond to maintain the pocket structure stable. From Cys2 to Cys11, they all are located in the N-terminal domain, and any of them mutated to Ser caused loss of almost all activity.

It should be noticed that the only difference between Cys and Ser is that the –SH group change to a –OH group; and the ability of form a disulfide bridges disappeared. Such phenomenon may lead to a conclusion that the accumulation of Cys In N-terminal domain was mainly to form a special stable structure. Such structure might require all Cys (except Cys1) in N-terminal domain, because ideally, 10 Cys could form 5 disulfide bonds and no free Cys left; and 5 disulfide bonds were enough to keep a stable structure. Due to Cys7 and Cys8 showed higher activity than other 8 Cys mutants, these two Cys (Cys38 and Cys47) might contribute to less important disulfide bond formation than other 8 Cys.

On the other hand, due to the fact that vitamin K epoxide reductase use two Cys in the active site (R.B.Silverman, 1981), it is tempting to suggest that cysteines in VDE is involved in catalysis. Because of the location of the active site of VDE is still unknown, investigation about whether the Cys in N-terminal contribute in catalitical way or structural way needs further work.

In 1998, Niyogi et al successfully isolated a natural *Arabidopsis thaliana* mutant that could not tolerate rapid light change. The mutant was named *npq1-1*. The mutation happened in *npq1-1* is the last Cys in Cys-rich domain (same position as in sample Cys11) mutates to Tyr. The mutant lost fully activity. We mutate the Cys at the same

place to Ser but in the different species (spinach), the result showed 0.1% of VDE3 activity was left. Compare with Tyr, the shape and property of Ser are much closer to Cys, the activity of mutants still decrease dramatically. Our result matches to the discovery from Niyogi's group.

In the linker function test, the activity of the 3 combinations were measured by the HPLC method due to the dual-wavelength method was insufficient to measure this low activity. This illustrate that the 6 peptides might not form correct folding independently or the collision between two domains into correct position required more time during the conversion reaction. It should be mentioned that in the beginning of activity assay by using HPLC method, the reaction was taken place in citrate-phosphate buffer, and we got very low amount of Vx conversion to Ax and Zx. After changing the citrate buffer to MES buffer at same pH by lower ion strength, the conversion of Vx to Ax and Zx was higher. This illustrate the salt in the activity assay buffer can influence the interaction between the two domains.

From the Figure 9, it should be noticed that the three small size peptides (L1, L3 and L5) showed different solubility. L1 is found in pellet, L3 can be found in both pellet and supernatant, L5 can only be found in supernatant. And from the result of activity assay, L5+L6 group showed higher activity than L3+L4 group while L1+L2 group gives no activity. We suggest that the three small size peptides have different ability to fold correctly and independently, or they have different solubility. And due to the dialysis method is lower efficient than the desalting column, it cannot completely remove urea. The refolding of L1 and L3 might not as complete as L5. And the L5 exist in soluble form after expression, it might remain more activity.

On the other hand, in the linker region (VPQKSDVGEFPVPDPSVLV), L1 and L2 were separated at position between Gln and Lys (QK), while the TEV-site was fused between position QK and FP; the low activity of the TEV-site fusion VDE and non-active peptide combination L1+L2 showed the real linker region should be smaller than what we suggested from the sequence alignment result (Figure 5). The sequence VPQKSDVGEF could have more functions than connecting the N-terminal and lipocalin domain. The successful cleavage of TEV-site fusion VDE showed that the linker region should be located in the surface of protein in VDE because the ACTEV protease cannot find and cleave the recognition sequence buried in protein. This also proved by the hydrophobicity plot by using ProtScale (Kyte & Doolittle scale, window size 3) prediction result. Such illustrated the linker region might be a loop structure with stable structure that can keep two domains connected and maintained in a certain angle.

The TEV-site fusion VDE was designed to detect if the two domains before and after the linker region were necessary to each other while folding. But the DTT in reaction buffer fully inhibited the VDE activity. The oxidative environment created by GSSG can fully remove the reducing power of DTT, but the step of mixed GSSG with

protease solution before the reaction highly reduced the activity of the protease; and on the other hand, the GSSG cannot remove the influence of DTT if GSSG was added after cleavage reaction. In conclusion, the solution to reduce the influence of DTT and at the same time keep the ACTEV protease active is to allow the protease cleave the TEV-site fusion protein and remove the DTT.

The activity measurement of the C-terminal-cleaved VDE3 showed that the truncated VDE3 lost activity. The longer distance C-terminal is removed, the less activity left. The truncated VDE3 with the whole C-terminal sequence removed (sample CR1) showed only about 0.2% of VDE3 activity. This result illustrated that besides the membrane binding function, which was suggested by Bugos and Yamamoto, the C-terminal might also influence the conversion of Vx to Ax and Zx or substrate binding function. Even though CR1 has low activity, it showed that the VDE3 without C-terminal was still able to convert from Vx to Ax and Zx. Therefore it would still be interesting to obtain the structure of CR1.

The research from A.D. Hieber et al (2001) showed that the truncated VDE from *Arabidopsis thaliana* with 278 amino acids (same size as CR3) shows full activity, and the 257 amino acid-length-VDE (7 amino acids more than CR1) showed no activity at all. But our experiment result showed some difference. Sample CR1 still shows a low activity while CR3 showed only 20% of full activity. The reason of such phenomenon might be our purification method is with higher efficiency than method in Hieber's group and spinach VDE is different from *Arabidopsis thaliana* VDE. The purification steps by using gel-filtration chromatography and desalting column produced high purity protein sample. The activity comparison of other sample to the high purity VDE3 is more accurate.

On the other hand, from Figure 15, it can be seen that the active oligomeric state of CR1 and VDE3 are different in high pH. CR1 can form active dimer in high pH, and was suggested that it might relate to the removal of 99 amino acid-C-terminal peptide. The C-terminal might influence the VDE3 molecule contacts to each other to form dimer at high pH. Due to our following discovery, the VDE3 forms dimer in low pH (Figure 13). Together with research of Bugos and Yamamoto in 1996, this process might be explained by that the low pH caused structural change of the C-terminal domain and induced its membrane binding function, and without the disturbance of C-terminal, other part of VDE formed dimer for conversion of Vx.

Figure 13 suggests the formation of VDE3 dimers at low pH. However, the 2 ml peak shift is not a reliable support of dimerization of VDE3 in low pH, besides the hight of VDE3 peak in low pH is only about 20% of that in the high pH which means around 80% of VDE3 sample were changed into insoluble form.

Another experiment was set up to reduce the reaction speed into a long time period and measure the conversion from Vx to Ax until Zx by using HPLC method. From our

prediction that the dimerization of VDE3 monomer would happen when the environment pH decreases to acidic state, if active VDE3 and non-active Cys11 were mixed together, the chance of VDE3 monomer form dimer with another VDE3 monomer decreased to half. The Figure 14E provided the evidence that support the dimerization of active VDE3: the diagram of the artificial doubled speed VDE3+Cys11 matched to the diagram of Figure 14A. The merged diagram showed the conversion speed of VDE+Cys11 is just the half of speed of VDE3.

In Figure 15, it can be seen that the peak of active CR1 sample appeared earlier than active VDE3 sample. The comparison of the position of the three peaks in each diagram shows CR1 should work in dimer form. The dimerization of CR1 even happened in high pH and the activity assay showed the monomer peak in CR1 diagram is inactive. Such phenomenon illustrated that VDE can dimerization at high pH without C-terminal region. In another word, C-terminal might influence the VDE activity in some other ways, but what we can confirm is it does influence the dimerization of VDE. But the domain that mainly contributed to the dimerization of VDE remains unknown.

In future work, a Circular Dichroism spectrum (CD spectrum) is suggested to analyze the folding of each Cys mutants to identify the Cys which contribute to VDE structure stability. Large scale TEV-protease digestion should be set up to prepare enough digestion products to load on PD-10 desalting column to remove DTT in the solution; the two active peptides will be loaded in low pH native gel electrophoresis to identify domain that contribute to dimer formation. The active short peptide L3 and would also be subjected to Nuclear Magnetic Resonance (NMR) method to obtain structure; at the same time, crystallization condition screens of CR1, CR2 and CR3 would be set up and further, obtain the structure.

Reference

Hager A, Holocher K. localization of the xanthophyll-cycle enzyme violaxanthin de-epoxidase within the thylakoid lumen and abolition of its mobility by a (light-dependent) pH decrease. (1994) Planta 192: 581-589

Gilmore Am, Yamamoto HY. Dark induction of zeaxanthin-dependent non-photochemical fluorescence quenching mediated by ATP. (1992) Proc Natl Acad Sci USA 89: 1899-903

P Arnoux, T Morosinotto, G Saga, R Bassi, D pignol. A structural basis of the pH-dependent xanthophyll cycle in *Arobidopsis thaliana*. (2009) The Plant Cell. Vol.21: 2036-2044

Bratt CE, Arvidsson P-O, Carlsson M, Åkerlund H-E. Regulation of violaxanthin de-epoxidase activity by pH and ascorbate concentration. (1995) Photosynth Res 45: 169-175

Gasteiger E., Hoogland C., Gattiker A., Duvaud S., Wilkins M.R., Appel R.D., Bairoch A. Protein Identification and Analysis Tools on the ExPASy Server;(In) John M. Walker (ed) (2005): The Proteomics Protocols Handbook, Humana Press. pp. 571-607

Bugos RC, Yamamoto HY. Molecular cloning of violaxanthin de-epoxidase from romaine lettuce and expression in *Escherichia coli*. (1996) ProcTatl Acad Sci USA 93: 6320-6325.

A. David Hieber, Robert C. Bugos, Amys. Verhoever, Harry Y, Yamamoto. Overexpression of Violaxanthin de-epoxidase: properties of C-terminal deletions on acting and pH dependent lipid-binding. (2001) Planta 214:476-483

Kyte J., Doolittle R.F. A Simple Method for Displaying the Hydropathic Character of a Protein. (1982) J. Mol. Biol. 157:105-132.

P. Müler, X.P. Li, K.K. Niyogi. Non-photochemical quenching. A response to excess light energy. (2001)Plant Physiology, Vol.125, pp. 1558-1566.

K.K.Niyogi, A.R. Grossman, O. Björkman. Arabidopsis mutants define a central role for the xanthophyll cycle in the regulation of photosynthesis energy conversion. (1998) The Plant Cell, vol. 10. 1121-1134.

Horton P, Hague A. Studies on the induction of chlorophyll fluorescence in isolated barley protoplasts: IV. Resolution of non-photochemical quenching. (1988) Biochim Biophys Acta 932: 107-115

Richard B. Silverman. Chemical model studies for the mechanism of vitamin K epoxide reductase. (1981) J. Am. Chem. Soc 103:5939-5941

H.Y. Yamamoto, R.M. Higashi. Violaxanthin de-epoxidase: lipid composition and substrate speceificity. Archives of Biochemistry And Biophysics vol.190, No.2, October, PP. 514-522. 1978.

H.Y. Yamamoto, Nakayama TOM, Chichester CO. Studies on the light interconversions of the leaf xanthophylls. (1962) Arch Biochem Biophys 97:168-173